RESEARCH PAPER

PCCP
www.rsc.org/pccp

A new infrared spectroscopy technique for structural studies of mass-selected neutral polar complexes without chromophore

Bruno Lucas, Frédéric Lecomte, Bernd Reimann, Hans-Dieter Barth, Gilles Grégoire, Yves Bouteiller, Jean-Pierre Schermann and Charles Desfrançois*

Laboratoire de Physique des Lasers, Institut Galilée, CNRS-Université Paris-Nord, Villetaneuse 93430, France. E-mail: desfranc@galilee.univ-paris13.fr; Fax: +33 1 4940 3200; Tel: +33 1 4940 3723

Received 9th December 2003, Accepted 20th January 2004
First published as an Advance Article on the web 10th February 2004

We report gas-phase experimental and theoretical results on the configurations of weakly-bound neutral polar complexes without chromophores: the water dimer and the formamide–water complex. Experimental data are obtained by combining infrared (IR) absorption spectroscopy, in the 2800–3800 cm^{-1} domain, with the Rydberg electron transfer (RET) technique leading to dipole-bound anion (DBA) formation. In the absence of IR excitation, RET to neutral complexes with a given total dipole moment, and thus a given molecular structure, leads to DBAs which are observed without any possible fragmentation. In the presence of the IR laser, prior to ionisation, resonant IR absorption of *intra*molecular vibrations of the parent neutral complexes can either induce the breaking of the weak *inter*molecular bonds (vibrational predissociation of the neutral) or the fast departure of the excess electron after RET (autodetachment of the DBA). Anion signal depletion, monitored at the parent mass, is then a signature of resonant IR absorption from mass- and structure-selected neutral complexes. The validity of the present experimental method and of different types of quantum chemistry calculations is discussed by comparison between calculated harmonic or anharmonic frequencies, the present experimental gas-phase IR spectra, and previous experimental data on these two test-case hydrogen-bonded complexes.

1. Introduction

We here present a new method for studying neutral molecular species in a beam, which combines the advantages of rigorous mass-selection with the beam depletion techniques for infrared (IR) spectroscopy.[1] Usually, IR spectroscopy of mass-selected neutrals is performed using the resonant two-photon ionisation (R2PI) technique.[2] In R2PI, a first tuneable UV laser selectively excites an electronic ($S_1 \leftarrow S_0$) transition of a molecular chromophore and a second laser ionises the selected neutral species, allowing for mass-spectrometric identification. In R2PI/IR,[2–5] a tuneable infrared laser beam is used for resonant excitation of intramolecular rovibrations of the neutral in the S_0 state. This IR absorption leads to a decrease of the neutral population in the ground rovibrational state and thus to a depletion of the cation signal at the parent mass. However, the absorbed excess energy can also induce vibrational predissociation, at least in the case of weakly-bound complexes.[6] Moreover, R2PI ionisation sometimes leads to fast fragmentation, so that the IR spectral information must sometimes be obtained at some daughter ion masses. Even if R2PI/IR is a very efficient method, which has provided a wealth of fundamental results,[4] it however requires the existence of a molecular chromophore with reasonably well-resolved and non-overlapping electronic spectra for specific neutral mass-selection.

In this work, we present an alternative method that is not universal but does not require the presence of a chromophore molecule in the investigated neutrals. The ionisation step is here performed by means of Rydberg electron transfer (RET) and relies on the capability of a polar molecular system, with large enough total dipole moment (>2 D), to weakly bind electrons (in the meV range). The produced dipole-bound anion (DBA) has an excess electron in a very diffuse orbital and most generally retains the geometry of its neutral parent. The main point is that this ionisation process almost does not feed any internal energy to the ionised species, so that ionisation is performed without any fragmentation, even for weakly bound complexes.[7] Another very important point is that the electron binding process is sensitive to the total dipole moment of the attaching neutral species and thus to its geometrical configuration. The RET ionisation process for DBA formation is thus also selective with respect to structural properties.[8] Mass-selection *and* structure-selection are thus accomplished in the same step.

However, different molecular configurations may correspond to similar total dipole moments so that discrimination may be impossible to perform by the measurement of only one molecular parameter. It was thus natural to combine this non-perturbative ionisation method with IR spectroscopy, in order to gain more information on molecular or complex structures. As for other beam depletion techniques, it was expected that IR absorption by neutrals must be detectable by a decrease in the corresponding DBA signals at the parent mass. IR absorption, in the mid-infrared region, indeed feeds the neutrals with an amount of internal energy (0.4 eV) that is larger than most of the dissociation energies of weakly-bound molecular complexes (0.1 to 0.3 eV) and much larger than DBA excess electron binding energies (0.01 eV). Thus, it must induce either the breaking of an intermolecular bond, *i.e.* the vibrational predissociation of the neutral parent complex, or the fast departure of the excess electron after RET anion formation, *i.e.* the vibrational autodetachment of the DBA. In the first case, IR absorption leading to vibrational predissociation has been proved to be efficient in many IR beam depletion studies of neutral complexes. In the second case, the efficiency of the anion autodetachment is more specific to the present ionisation technique and may be more

DOI: 10.1039/b316054h

hypothetical since, in DBAs, the excess electron does not interact too much with the neutral core. However, vibrational autodetachment has been observed for molecules vibrationally excited and electronically excited in Rydberg states. Since Rydberg molecules constitute neutral counterparts of DBAs, vibrational autodetachment is also expected in that case. In both cases, we thus expect a decrease of the DBA signals either due to beam depletion of the neutral parents or due to the disappearance of anions after RET.

We first recall the main experimental features of IR excitation and RET ionisation steps, and then present experimental data concerning two simple test-case dimers without chromophores. The water dimer is a well-studied system that we consider in order to validate the present new experimental technique. The formamide–water complex is a very simple model system for the hydration of the peptide bond and it has been previously studied only in argon matrix.[9] Both species can be considered as benchmark systems for a comparison with accurate quantum chemistry calculations for hydrogen bonded complexes.

2. Experimental

A pulsed supersonic beam of water–formamide neutral complexes is produced by flowing 1.5 bar of helium over a water reservoir, slightly heated at 35 °C, followed by a formamide reservoir heated at 80 °C. This gas mixture is expanded under vacuum through a heated pulsed valve (General Valve; 0.15 mm conical nozzle; $T > 80$ °C) followed, 1 cm downstream, by a skimmer of 2 mm diameter. In the case of water dimers, the formamide reservoir is removed and the entire line is kept at room temperature. This supersonic beam penetrates the acceleration region of a Wiley–McLaren time-of-flight set-up and is first crossed at right angles with a mildly focused IR beam produced by a seeded pulsed (few ns) OPO laser.

This homemade OPO set-up has been built according to the design developed at the University of Frankfurt.[6] A seed optical signal around 3 μm is produced by mixing 7 mJ at 532 nm, from a non-injected YAG laser (Brillant B from Quantel), with 5 mJ at 620–670 nm, produced by a tuneable dye laser pumped by the same YAG laser second harmonic. This difference frequency mixing is performed in a first $LiNbO_3$ crystal and gives few tens of μJ of IR light that is used to inject an OPO laser cavity. A second crystal is thus pumped by 130 mJ of a 1.06 μm laser beam, still from the same YAG laser and withdrawn before frequency doubling. A good beam profile is obtained by imaging the output beam profile onto the cavity $LiNbO_3$ crystal, using a set of lenses and a small vacuum chamber (around the focalisation point) along the 3.5 m long pump–beam path. The OPO laser cavity is 12 cm long and is resonant with respect to the signal radiation (1.5–1.8 μm). The typical idler output (2.6–3.7 μm) is 2–5 mJ at the OPO exit and 1–3 mJ in the interaction region, with an IR laser beam diameter of about 2 mm. The practical tuneable range covers the whole 2600–3900 cm^{-1} region except for a dip in between 3460 and 3510 cm^{-1} that is due to OH impurities in the crystals. The fundamental of the YAG (1.06 μm), its second harmonic (532 nm) and the dye laser have respective line widths of 0.7, 1.4 and less than 0.1 cm^{-1}, leading to an estimated line width of 1.5 cm^{-1} for the IR light. This OPO laser has been first calibrated by measuring different dye laser wavelength, with a high-precision lambdameter, in order to obtain the calibration curve, as a function of the number of dye motor steps. Subsequent calibration has also been performed on two series of xenon *n*d and *n*g Rydberg states, excited by the OPO laser from the 6f Rydberg state. These calibration tests confirmed the laser line width (2 cm^{-1}) and led to an estimation of the absolute frequency precision of about 1 cm^{-1}.

After IR excitation, the neutral complexes are ionised by further crossing a beam of metastable xenon atoms which are excited towards *n*f Rydberg states by means of a visible pulsed laser (460–520 nm) in the same region. The visible laser beam diameter in this collision region is about 1 mm and the distance between the two collinear laser beams is about 3 mm. The visible laser pulse is delayed by 200 ns after the IR laser pulse. Electron transfer collisions take place between the Rydberg atoms and the cold neutral complexes, leading to DBAs that are extracted after an additional time delay of 2 μs to allow for the building of the anion population. Rydberg atoms can indeed have large radiative lifetimes (up to few μs in the present experiments) during which anions are continuously produced. The anions are then accelerated, focused and sent into the time-of-flight tube, at the end of which they are detected as a function of time. As shown in many previous experiments, the RET-DBA formation rates are strongly dependent upon the principal quantum number n of the Rydberg atoms.[10] In the present experiments, we maximize the anion formation rates, by setting the Rydberg n values at $n = 24$ for the formamide–water complex,[11] and at $n = 13$ for the water dimer.[12] In the first case, the very low excess electron energy (3.1 meV[11]) of the observed formamide–water DBAs requires the lowering of the extraction and acceleration fields in the time-of-flight set-up, in order to avoid field-detachment.

The IR laser is run at 10 Hz while the visible laser operates at 20 Hz so that we can perform real-time on–off subtraction of two consecutive signals. In the present experimental set-up, the main difficulty, with respect to IR spectroscopic purposes, is indeed the weakness of the anion signals. Typical DBA signals are 0.1 per laser shot for water dimers and four times weaker for formamide–water complexes. In order to obtain good statistics we thus have to accumulate signals during at least 2000 laser shots (200 s), for the water dimer, and four times more (800 s), for the formamide–water complex, at each wavelength. A scan over 100 cm^{-1}, with 1 cm^{-1} steps, can thus represent several tens of hours of experiments. Moreover, in order to further increase the signal-to-noise ratio, all scans have been repeated three times and the resulting spectra thus correspond to the average of three independent experiments. The total collection time was thus about one month for each complex.

3. Results

Formamide–water and water dimer anions are thus prepared by RET charge-exchange collisions between cold neutral complexes and laser-excited *n*f Rydberg atoms, with n respectively equal to 24 and 13. The depletion of anion signals at the parent masses is then recorded by scanning the IR OPO laser through the different intramolecular vibrational absorption regions. Experimental IR absorption spectra, obtained with this technique for the neutral water dimer and the formamide–water complex are displayed in Fig. 1 and 2. In these figures, small dots correspond to the average value of three independent measurements and thick lines correspond to a smooth over three adjacent points. This leads to a better view of the spectra, which are otherwise still quite noisy. The typical DBA signal fluctuations are indeed of the order of 10% while observed depletion are between 10 and 40%.

For the water dimer, we clearly observe a strong (30% of depletion) and broad (FWHM of 11 cm^{-1}) absorption lines in the region of the bonded O–H stretch. This large line width is probably due to saturation. In the region of the free O–H bands, we clearly observe one weaker (20–30% of depletion) and narrower (FWHM of 6 cm^{-1}) line and a second, smaller but reproducible, line at a slightly larger frequency. The experimental values of these observed O–H absorption band positions for the water dimer are reported in Table 1, in comparison with previous experimental data obtained in argon matrix[13] and by beam depletion either on unselected neutrals[14]

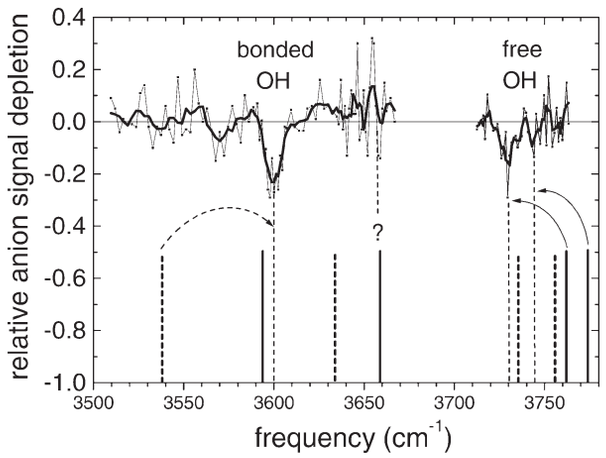

Fig. 1 IR spectrum of the mass-selected neutral water dimer obtained from DBA signal depletion. Small squares correspond to relative depletion values averaged over three independent measurements while full thick lines correspond to a smooth over three adjacent points. Experimental line positions are indicated by thin dash lines and theoretical frequencies are located by full (anharmonic) or dash (scaled harmonic) bars. The question mark corresponds to the position of the fourth line, expected from matrix data. See text for discussion.

or on partially selected clusters.[15] Within our spectral resolution, the present data are in very good agreement with those previous studies. This is particularly true for the comparison with high resolution Miller's data[14] since our values differ only by 2 cm^{-1} for the acceptor asymmetric stretch. We must however recall that the lack of mass selection in Miller's experiments led to a wrong assignment of the band at 3600 cm^{-1}. The correct assignment of this band has been given later by Huisken using the cluster selection technique with helium beam deflection.[15] However, this technique also suffers from some contamination of larger water clusters, so that it was not possible to resolve the two O–H absorption bands at 3735 cm^{-1}. The present data thus constitute the first observation of all these three O–H bands in water dimers rigorously mass-selected in a beam. The fourth acceptor symmetric O–H band has been only observed in argon matrix experiments due to its weak intensity. As compared to beam data, those matrix data[13] are, as expected, systematically red-shifted by about -20 cm^{-1}. The fourth band is thus expected to be very close to 3657 cm^{-1}, for gas-phase water dimers, but, despite a careful search, we did not observe any sizeable signal depletion in this region (see the question mark in Fig. 1).

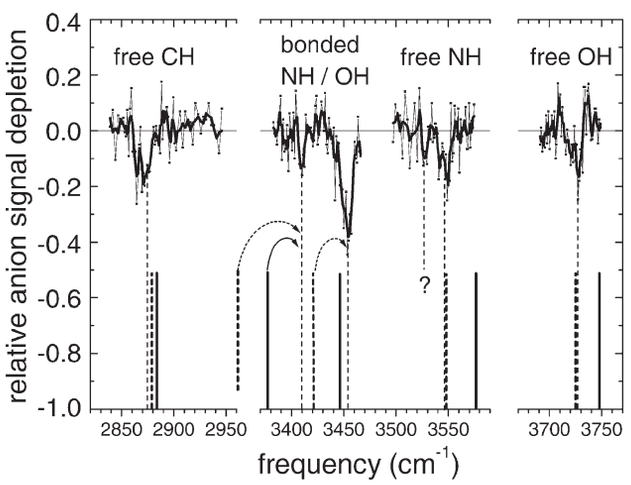

Fig. 2 As in Fig. 1 for mass-selected neutral formamide–water complex. The question mark corresponds to a line which is not assigned. See text for discussion.

Table 1 IR O–H absorption band frequencies (cm^{-1}) for water dimers, as measured in previous experiments and in the present work

O–H absorption	Argon matrix Ref. 13	Beam depletion Ref. 14	Cluster selection Ref. 15	DBA-RET-IR present work
Acceptor asymmetric	3726	3745	3735	3743
Donor free	3709	3730		3730
Acceptor symmetric	3634	—	—	—
Donor bonded	3574	3600	3601	3600

For the formamide–water complex, we were able to observe the five stretch vibration absorption lines. They correspond to DBA depletions between 15 and 40% in the order bonded N–H < free C–H ~ free N–H ~ free O–H < bonded O–H, in good agreement with what was expected from intensity calculations (see below). Again, the bonded O–H line is broader (12 cm^{-1}) than the other lines, probably because of saturation. However, all three free stretch lines seem to be split, with a smaller peak appearing 6 to 10 cm^{-1} below the main peak. At the present time, we have no interpretation of this splitting. Furthermore, there is also a third additional small peak about 20 cm^{-1} below the main free N–H line (see the question mark in Fig. 2). Again, no clear explanation can be given now, even if a possible Fermi resonance could be invoked between the free N–H and O–H lines and one low-frequency mode. In Table 2, we compare the present results for isolated water–formamide dimers to the only previous experimental data from matrix measurements.[9] Again, these matrix data are systematically red-shifted by -19 to -26 cm^{-1}, except for the C–H stretch for which the observed shift is $+13$ cm^{-1} in the blue. The same matrix red shift as for the other absorption bands would have led to a gas-phase band position at about 2905 cm^{-1}, for the C–H stretch, but a careful inspection of this region did not display any signal depletion. The reason is not clear for this difference between the C–H and the other bond stretch absorption bands but it also arises in the case of the formamide monomer. In this molecule, both the symmetric and asymmetric N–H stretch are red-shifted by about -10 cm^{-1}, in the matrix data as compared to the gas-phase data, while the C–H stretch is blue-shifted by about $+20$ cm^{-1}.[16]

4. Calculations and discussion

During the last decade, theoretical chemists have strongly improved the accuracy of predictions of vibrational frequencies,[17–19] although some important problems remain, in particular in the case of hydrogen-bonded complexes. We here wish to use our experimental results as benchmarks for *ab initio* theoretical calculations, as experimentalists can run them on a personal computer and with commercial software. We thus establish a comparison between calculated harmonic and

Table 2 IR absorption band frequencies (cm^{-1}) for the formamide–water complex, as measured in argon matrix experiments and in the present work

IR absorption	Argon matrix [9]	DBA-RET-IR present work
Free O–H	3707	3727
Free N–H	3522	3548
Bonded O–H	3430	3454
Bonded N–H	3391	3410
C–H	2887	2874

anharmonic frequencies and the present experimental gas-phase IR spectra. We present MP2 calculation results obtained with a quite large basis set, 6-31++G(2d,2p), using the Gaussian03W software package,[20] which has been run on a 2.2 GHz AMD Athlon processor. The calculation procedure is the following. Since the lowest equilibrium geometry of both the water dimer and the formamide–water complex are well established[11] (see Scheme 1), we start from these structures and we run, at the above given level of theory, a full structure optimisation, without any symmetry constraint, followed by harmonic and anharmonic frequency calculations. The same calculations are also performed on the monomers in order to determine the harmonic scaling factors for the different vibrational frequencies of formamide and water. We then take the average values of these monomer scaling factors, *i.e.* 0.9472 for the water O–H vibrations and 0.9447 for the formamide N–H and C–H vibrations, for the scaling of the harmonic frequencies obtained for the dimers. Those results are displayed in Table 3 for the monomers and in Table 4 for the dimers, where the deviations $\Delta\nu$ from experimental values and the frequency shifts between free and bonded stretch vibrations are also indicated.

For monomers, as expected, the calculated anharmonic values are much closer to the experimental data than the non-scaled harmonic values (see Table 3). This is particularly true for the water O–H and the formamide C–H vibrations, for which the absolute anharmonic values deviate from the experimental values by only $\Delta\nu \sim +10/+30$ cm^{-1}. On the other hand, $\Delta\nu$ increases up to $+57/+80$ cm^{-1} for the two formamide N–H stretch frequencies. This discrepancy is probably due to the difficulty in fully taking into account the highly anharmonic couplings of the N–H stretch vibrations with the low-frequency out-of-plane mode of the two N–H bonds (harmonic value of 183 cm^{-1}). As a consequence, the mean square displacement (MSD) between anharmonic and experimental data, for the five considered stretch vibrations, is about 47 cm^{-1} (24 cm^{-1} for water, 57 cm^{-1} for formamide).

For dimers, anharmonic calculations also perform quite well and slightly better than scaled harmonic calculations and also even better than for monomers (see Table 4). The MSD between anharmonic and experimental frequencies is indeed 22 cm^{-1} while the MSD between scaled harmonic and experimental values is 34 cm^{-1}, either for the four water dimer stretch modes or for the five formamide–water modes or for both of them. In particular, the anharmonic deviation value is only -7 cm^{-1} for the bonded O–H, in both dimers, and -33 cm^{-1} for the bonded N–H. Even the free N–H vibration in formamide–water comes in better agreement with the experimental result than in the formamide monomer ($+28$ cm^{-1} instead of $+80$ and $+57$ cm^{-1}). Again, this may be explained by the fact that the out-of-plane mode of the two N–H bonds is hindered by the presence of the water molecule, which forms a double hydrogen bond between one formamide N–H bond, as a proton acceptor, and the formamide C=O bond, as a proton donor. In comparison with anharmonic results, the corresponding scaled harmonic deviations are much higher for the three bonded O–H and N–H vibrations ($\Delta\nu$ values of -62, -33 and -70 cm^{-1}) but they are better for the six free stretch modes ($\Delta\nu$ in between -24 and $+13$ cm^{-1}). This is not surprising since the scaling procedure is expected to be rather inaccurate in taking into account the anharmonic couplings between inter- and intra-molecular bonds, while it is designed to fit the experimental free stretch modes.

It is also interesting to have a look at the frequency shifts between the free and bonded stretch vibrations (values in parentheses in Table 4). In the water dimer, the bonded O–H is experimentally red-shifted by 130 cm^{-1} while harmonic calculations always lead to larger red shifts.[21] In the present work, the harmonic red shift is indeed 209 cm^{-1} and is only slightly reduced to 198 cm^{-1} by the scaling procedure. Anharmonic calculations perform better since the red shift is further reduced to 169 cm^{-1}, but still about 40 cm^{-1} larger than the experimental value. Similar results have been previously obtained either from anharmonic calculations[22] or from high-level (CCSD(T)) *ab initio* calculations with large basis sets.[17] It could thus be expected that using both high-level methods and basis sets and anharmonic calculations would lead to really accurate absolute frequency values, for hydrogen bond complexes, but this is still to be done and reserved to very small species, such as the water dimer. For the formamide–water complex, the bonded O–H and N–H stretch are experimentally red-shifted by respectively 273 and 138 cm^{-1}. Again non-scaled and scaled harmonic red shifts are too large, *i.e.* respectively about 310 and 210 cm^{-1}. In that case, the anharmonic calculations do not perform much better, with red-shifts respectively equal to 300 and 199 cm^{-1}, *i.e.* too large by 27 and 61 cm^{-1}. As compared to the previous discussion about the deviations with respect to experimental data, the situation here appears to be less encouraging. The reason why the deviations from experiment are smaller for anharmonic calculations, is not only due to more accurate frequency shifts of the bonded stretch vibrations. It is also the result of an overall blue-shift of

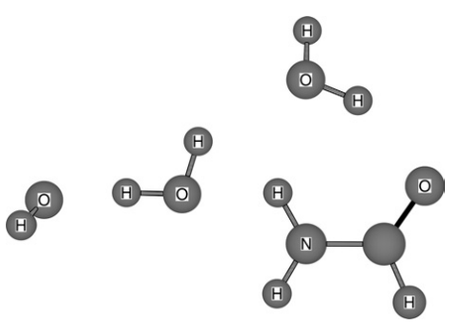

Scheme 1 Equilibrium structures of the water dimer and the formamide–water complex.

Table 3 Gas-phase experimental and calculated (MP2/6-31++G(2d,2p)) harmonic and anharmonic vibrational frequencies (cm^{-1}) for the water and formamide molecules. Deviations from experimental values $\Delta\nu$ (cm^{-1}), harmonic scaling factors and computed band intensities (km mol^{-1}) are also given

Molecule	Vibration	Exp. frequency[23,24]	$\Delta\nu$	Calc. anharmonic frequency	Calc. harmonic frequency	Harmonic scaling factor	Calc. intensity
Water	Asym. O–H stretch	3756	+32	3788	3980	0.9437	67
	Sym. O–H stretch	3657	+11	3668	3847	0.9506	9
Formamide	Asym. N–H stretch	3564	+80	3644	3784	0.9419	59
	Sym. N–H stretch	3439	+57	3496	3629	0.9476	50
	C–H stretch	2854	+12	2866	3021	0.9447	84

Table 4 Present results for the gas-phase experimental and calculated (MP2/6-31++G(2d,2p) anharmonic and scaled harmonic vibrational frequencies (cm^{-1}) for the water dimer and the formamide–water complex. The harmonic scaling factors used are those given in Table 3 (see text) and calculated intensities (km mol^{-1}) are also given, together with the deviations from experimental values $\Delta\nu$ (cm^{-1}). The shifts (cm^{-1}) between free and bonded stretch vibrations are given in parentheses

Species	Vibration	Exp. frequency	$\Delta\nu$	Calc. anharmonic frequency	$\Delta\nu$	Scaled harmonic frequency	Harmonic frequency	Calc. intensity
Water dimer	Acceptor asymmetric O–H	3743	+30	3773	+13	3756	3965	91
	Donor free O–H	3730	+32	3762	+6	3736	3944	107
	Acceptor symmetric O–H	3657[a]	+2	3659	−24	3633	3836	16
	Donor bonded O–H	3600 (−130)	−7	3593 (−169)	−62	3538 (−198)	3735 (−209)	304
Formamide–water complex	Free O–H	3727	+20	3747	−3	3724	3932	93
	Free N–H	3548	+28	3576	+1	3549	3757	120
	Bonded O–H	3454 (−273)	−7	3447 (−300)	−33	3421 (−303)	3612 (−320)	442
	Bonded N–H	3410 (−138)	−33	3377 (−199)	−70	3340 (−209)	3535 (−222)	60
	Free C–H	2874	+9	2883	+6	2880	3049	84

[a] Expected value from matrix data[13].

all stretch frequencies, especially in the case of the formamide–water complex.

5. Summary and conclusions

In this paper, we demonstrate the feasibility of an original experimental technique, which enables IR spectroscopic studies on rigorously mass-selected neutral polar weakly-bound complexes, without the need of a molecular chromophore. Experimental data, obtained on the water dimer and the formamide–water complex, show very good agreement with previous gas-phase and matrix studies. They are used as benchmarks for a test of scaled harmonic and anharmonic *ab initio* frequency calculations, in the case of simple hydrogen-bonded species. Anharmonic results are found to be better than scaled harmonic results because they give slightly better absolute values without any empirical parameter. However, it seems that absolute accuracies better than about 30 cm^{-1} could be obtained only by using both high-level methods (better than MP2, with large basis sets) and anharmonic frequency calculations.

Future studies will concern polar simple molecules and larger complexes. One short-term development of the experimental set-up will be to greatly improve the DBA production by replacing the xenon Rydberg atom beam by an alkali atom beam with a two-colour laser excitation scheme. Then it would be possible to replace the present heated cluster beam valve by a matrix-assisted laser desorption source in a supersonic beam, in order to study molecules and molecular complexes of biological interest.

Acknowledgements

The authors would like to acknowledge Prof. Bernhard Brutschy for his stimulating advice and Olivier Lopez and Marc Barbier for their kind technical help in building the IR OPO laser.

References

1 K. Nauta and R. E. Miller, *Science*, 1999, **283**, 1895.
2 E. G. Robertson and J. P. Simons, *Phys. Chem. Chem. Phys.*, 2001, **1**, 1.
3 J. R. Carney, F. C. Hagemeister and T. S. Zwier, *J. Chem. Phys.*, 1998, **108**, 3379.
4 B. Brutschy, *Chem. Rev.*, 2000, **100**, 3891.
5 M. Gerhards, C. Unterberg and A. Gerlach, *Phys. Chem. Chem. Phys.*, 2002, **4**, 5563.
6 B. Reimann, K. Buchhold, H. D. Barth, B. Brutschy, P. Tarakeshwar and K. S. Kim, *J. Chem. Phys*, 2002, **117**, 1.
7 C. Desfrançois, H. Abdoul-Carime and J. P. Schermann, *Int. J. Mod. Phys.*, 1996, **10**, 1339.
8 C. Desfrançois, H. Abdoul-Carime, C. P. Schulz and J. P. Schermann, *Science*, 1995, **269**, 1707.
9 A. Engdahl, B. Nelander and P. O. Astrand, *J. Chem. Phys.*, 1993, **99**, 4894–4907.
10 C. Desfrançois, *Phys. Rev. A*, 1995, **51**, 3667.
11 F. Lecomte, B. Lucas, G. Grégoire, J. P. Schermann and C. Desfrançois, *Eur. Phys. J. D*, 2002, **20**, 449.
12 C. Desfrançois, A. Lisfi and J. P. Schermann, *Z. Phys. D*, 1992, **24**, 297.
13 R. M. Bentwood, A. J. Barnes and W. J. Orville-Thomas, *J. Mol. Spectrosc.*, 1980, **84**, 391.
14 Z. S. Huang and R. E. Miller, *J. Chem. Phys.*, 1989, **91**, 6613.
15 F. Huisken, M. Kaloudis and A. Kulcke, *J. Chem. Phys.*, 1996, **104**, 17.
16 S. T. King, *J. Phys. Chem.*, 1971, **75**, 405.
17 J. Kim, J. Y. Lee, S. Lee, B. J. Mhin and K. S. Kim, *J. Chem. Phys.*, 1995, **102**, 310.
18 P. Tarakeshwar and S. K. Kim, *J. Mol. Struct.*, 2002, **615**, 227.
19 J. Neugebauer and B. Hess, *J. Chem. Phys.*, 2003, **118**, 7215.
20 *Gaussian 03*, M. J. Frisch, G. W. Trucks, H. B. Schlegel, G. E. Scuseria, M. A. Robb, J. R. Cheeseman, J. A. Montgomery, Jr., T. Vreven, K. N. Kudin, J. C. Burant, J. M. Millam, S. S. Iyengar, J. Tomasi, V. Barone, B. Mennucci, M. Cossi, G. Scalmani, N. Rega and G. A. Pet, 2003.
21 J. Kim, J. Y. Lee, K. S. Oh, J. M. Park, S. Lee and K. S. Kim, *Phys. Rev. A*, 1999, **59**, 930.
22 A. Bleiber and J. Sauer, *Chem. Phys. Lett.*, 1995, **238**, 243.
23 *Chemistry WebBook Standard Reference Database 69*, NIST, 2003.
24 D. McNaughton, C. J. Evans, S. Lane, C. J. Lane and J. Nielsen, *J. Mol. Spectrosc.*, 1999, **193**, 104.

